JOURNAL OF MATERIALS SCIENCE 17 (1982) 970–978

Approximate methods to analyse non-linear creep behaviour and their application to some special materials

M. PARTL, C. TINIÇ, A. RÖSLI
Institut für Baustoffe, Werkstoffchemie und Korrosion, Swiss Federal Institute of Technology, ETH-Hönggerberg, CH-8093 Zürich, Switzerland

In this paper two approximate methods for the prediction of the non-linear time-dependent behaviour of poured asphalt and European spruce (*Picea abies* (*L*) *Karst.*) in uniaxial compression creep-tests at constant temperature are described. It is shown that the application of these two methods to several arbitrary step-loading and repeated single-step loading histories leads to a fairly good agreement between the prediction and the experimental data.

1. Introduction

The mechanical behaviour of many technologically important materials cannot be described sufficiently by the classical theory of elasticity which implies that the current strain is uniquely determined by the actual stress. This also applies to the investigated materials poured asphalt and European spruce, which, in addition to the properties of elastic solids, show the time-dependent behaviour of viscous fluids, and thus, a decreasing tendency to recover their original undeformed state after unloading. Consequently, the current strain depends not only on the actual stress-condition, but also according to the material memory, on the past loading-history.

A distinction can be drawn between visco-elastic bodies and visco-plastic bodies, where reloading is connected with hardening. In addition, materials such as poured asphalt are subject to ageing processes which are caused by chemical and structural changes and usually lead to a reduction of viscous behaviour [1].

The consideration of all influences by general constitutive equations leads to complex problems both theoretically and experimentally [2–5]. In practice, the calculations soon become unwieldy, if temperature and possible non-linearities are taken into account. Hence, various approximate and simple models (e.g., rheological models) are used for practical purposes.

In this paper the two approximate methods of analysing time-dependence developed in [6] and [7] are discussed in detail and compared with the experimental creep data of the materials mentioned above. The methods are valid for the primary and secondary stages. It is shown (see Figs 3 to 6) that both methods give a qualitatively and quantitatively good prediction of the long-time behaviour of the materials investigated herein.

2. Theory

The magnitude of deformations is influenced by the structure of materials, the applied load, the loading time and the temperature. Most building materials behave as solids and fluids as well, and therefore, they show both time-dependent and time-independent reversible and irreversible behaviour.

With higher number of loadings the contribution of each cycle to the total irreversible deformation decreases [7] and the material gradually loses its initial properties. Since in most cases it is not only the initial but also the N^{th} loading that is of great importance, it is of practical interest to be able to predict the long-time behaviour under repeated loading by using the material properties of single-step tests.

The creep history due to single step loading can be expressed for non-linear materials by

 0022–2461/82/040970–09$03.58/0

$$\epsilon(t) = \Phi_1(t)\sigma + \Phi_2(t)\sigma^2 \qquad (1)$$

or the creep compliance

$$\frac{\epsilon(t)}{\sigma} = \Phi_1(t) + \Phi_2(t)\sigma, \qquad (2)$$

which depends on the stress, σ. $\Phi_1(t)$ and $\Phi_2(t)$ are the time- and temperature-dependent material functions and have to be determined from experiments. In the following two approximate methods $\Phi_1(t, T)$ and $\Phi_2(t, T)$ are generally expressed by power functions.

2.1. Method 1

This method [6] is mainly based on the separation of the strain [8] into a reversible elastic and visco-elastic part (Fig. 1c) as well as into an irreversible plastic and visco-plastic part (Fig. 1d); furthermore, on the separate superposition of these parts by considering non-linear material behaviour and, by assuming hardening for plastic–visco-plastic parts in case of repeated loading (Fig. 2).

The separation is based on the assumption that the loading time, τ, equals the recovery time, $2\tau - \tau$, and that the time dependent and independent reversible parts can be determined at $t = \tau$ and $t = 2\tau$, respectively. Furthermore it is implied that the remaining strain consists of a time-dependent and time-independent part.

As it is seen in Fig. 1, the total strain, ϵ_g, can be split into four separate strain parts resulting from the first loading and unloading cycle

$$\epsilon_g = \epsilon_{ge} + \epsilon_{gp} = \epsilon_e + \epsilon_{ve}(t) + \epsilon_p + \epsilon_{vp}(t). \qquad (3)$$

According to Equation 1 each part can be expressed by individual polynomials with the material functions $\Phi(t)$ for constant temperature and the stress, σ. By inserting $\Phi_i(t) = \hat{\Phi}_i t^q$, Equation 3 can be transformed to

$$\epsilon_g = \hat{\Phi}_{1e}\sigma + \hat{\Phi}_{2e}\sigma^2 + \hat{\Phi}_{1ve}\sigma t^{q_{ve}} + \hat{\Phi}_{2ve}\sigma^2 t^{q_{ve}} + \hat{\Phi}_{1p}\sigma + \hat{\Phi}_{2p}\sigma^2 + \hat{\Phi}_{1vp}\sigma t^{q_{vp}} + \hat{\Phi}_{2vp}\sigma^2 t^{q_{vp}}, \qquad (4)$$

with $\hat{\Phi}_{1e} \ldots q_{ve} \ldots$ denoting ten material constants resulting from experiments (see Table IA). Factoring out $t^{q_{ve}}$ and $t^{q_{vp}}$ in Equation 4 and introducing the reversible parts

$$\hat{\epsilon}_e = \hat{\Phi}_{1e}\sigma + \hat{\Phi}_{2e}\sigma^2 \qquad (5)$$

and

$$\hat{\epsilon}_{ve} = \hat{\Phi}_{1ve}\sigma + \hat{\Phi}_{2ve}\sigma^2, \qquad (6)$$

and the irreversible parts

$$\hat{\epsilon}_p = \hat{\Phi}_{1p}\sigma + \hat{\Phi}_{2p}\sigma^2 \qquad (7)$$

and

$$\hat{\epsilon}_{vp} = \hat{\Phi}_{1vp}\sigma + \hat{\Phi}_{2vp}\sigma^2 \qquad (8)$$

the equation finally becomes (see Table IIB)

$$\epsilon_g = \hat{\epsilon}_e + \hat{\epsilon}_{ve} t^{q_{ve}} + \hat{\epsilon}_p + \hat{\epsilon}_{vp} t^{q_{vp}}. \qquad (9)$$

With the material constants of Equation 4 from single-step creep and recovery experiments it is possible to describe the material behaviour under repetitive loading, using a similar method as Lai and Anderson [9] who determined reversible strain with the modified superposition principle of Findley *et al.* [10, 11] and irreversible strain with a strain-hardening theory. The difference of the method presented in our paper consists in another treatment of the plastic and visco-plastic parts.

Compared to a single step-loading in the time interval $t = 0$ to $t = \tau$, the irreversible strain under repeated loading shows a greater increase in the same time interval. With higher number of cycles, N, this tendency seems to lead to a limiting value (Fig. 3). In the time-dependent visco-plastic parts, the strains increase only under loading. In case of

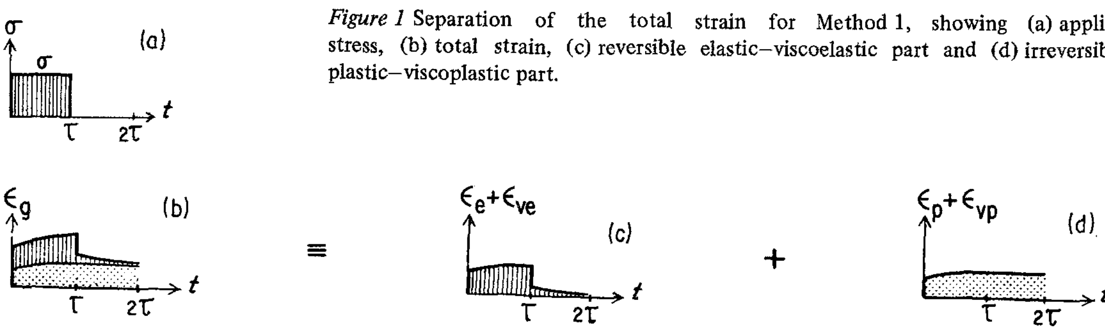

Figure 1 Separation of the total strain for Method 1, showing (a) applied stress, (b) total strain, (c) reversible elastic–viscoelastic part and (d) irreversible plastic–viscoplastic part.

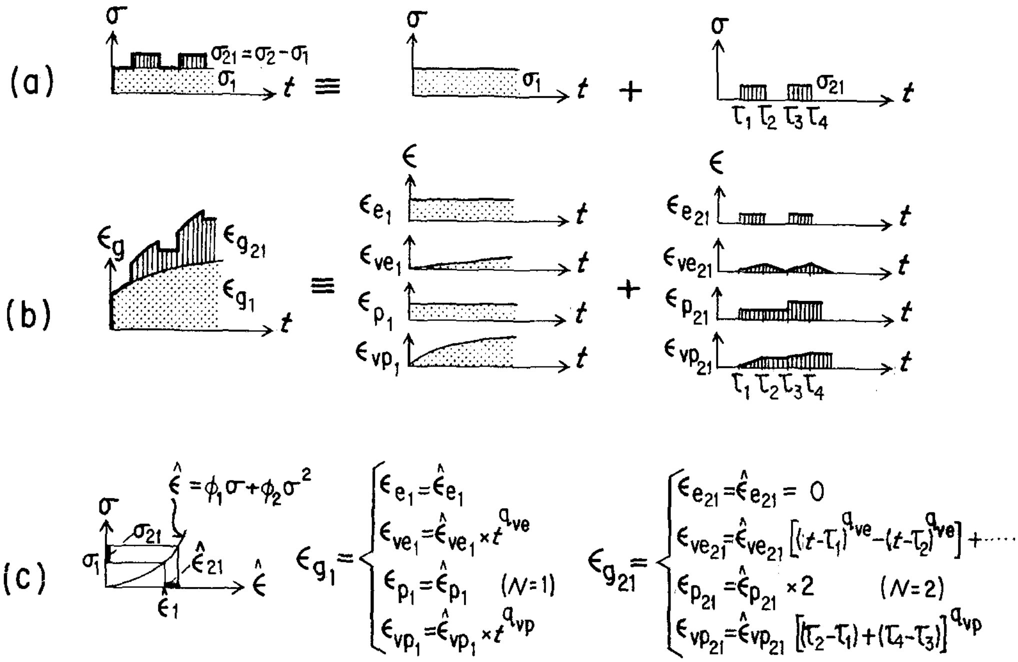

Figure 2 Example of the superposition according to Method 1. (a) Separation of the stress history in σ_1 and $\sigma_2 - \sigma_1 = \sigma_{21}$; (b) separation of total strain according to Fig. 1 and Fig. 2c; (c) determination of non-linear constants $\hat{\epsilon} \ldots, q \ldots$ (Table II) and calculation of total strain ϵ_{g_1} and $\epsilon_{g_{21}}$ with modified superposition for the elastic and visco-elastic part and Equations 10 and 11 for the plastic and visco-plastic part.

unloading the visco-plastic strain remains stable until the next load is applied. Consequently, only the effective loading period, τ, of every loading cycle must be considered, and it follows that

$$\epsilon_{vp} = \hat{\epsilon}_{vp}(N\tau)^{q_{vp}}. \tag{10}$$

In this equation, the time, τ, for $N = 1$ must tend towards zero and $\hat{\epsilon}_{vp}$ towards $\hat{\epsilon}_p$ for very short loading periods. By choosing $\tau = 1 - 1/N$ instead of $\tau = 0$ which is also zero for $N = 1$, the dependence of ϵ_p on the number of loadings N and on the initial material parameters q_{vp} and $\hat{\epsilon}_p$ can be described by the following relation

$$\epsilon_p = \hat{\epsilon}_p[1 + (N-1)^{q_{vp}}], \tag{11}$$

where $\epsilon_p = \hat{\epsilon}_p$ stands for the time-independent plastic part of the first loading cycle $N = 1$.

The example below shows the application of the single-step model to arbitrary step-loading histories by using this superposition method (Fig. 2).

The loading or unloading is expressed by the stress incremental $(\sigma_2 - \sigma_1)$ at $t = \tau_1$, and the resulting material parameter is obtained by the difference of the parameters for $\sigma_2 - \sigma_1$ (Fig. 2).

If the unloading history is split (as shown in Fig. 2a) and the Equations 5 and 6, 7 and 8 and 9, together with the corresponding material parameters, are applied to the response of every single-step loading increment, the material behaviour can be predicted with sufficient accuracy by the superposition of each part. This has been demonstrated by these (Figs 3 to 6) and earlier [12] experiments.

2.2. Method 2

The isothermal material behaviour can also be predicted by another separation of the total deformation [8]. This method is based on the frequent experimental observation (Fig. 7) of a difference ϵ_{ir} between the strain increments at the spontaneous loading and unloading times $t = 0$ and $t = \tau$, which decreases with repeated loading cycles (Fig. 3), and, furthermore, on the experience that, in many cases the modified superposition principle [10, 11] overestimates the recovery strain. Therefore, the total strain ϵ_g is split into the spontaneous strain, ϵ_{ir}, and the time-dependent part, ϵ_m, determined by the modified superposition principle. In the recovery period $2\tau - \tau$, the strain difference $\bar{\epsilon}_r$ remains, characterising the resistance against recovery.

TABLE IIA Tabulation of the stress dependent values for Method 1 (e.g., Equation 5 to 8)

Material	σ (N mm^{-2})	$\hat{\epsilon}_e$ (% at t = 1 sec)	$\hat{\epsilon}_{ve}$ (% at t = 1 sec)	$\hat{\epsilon}_p$ (% at t = 1 sec)	$\hat{\epsilon}_{vp}$ (% at t = 1 sec)	q_{ve}	q_{vp}
Poured asphalt	0.2	0.280	0.132	0.720	0.248	0.278	0.340
	0.4	0.370	0.162	0.910	0.425		
Spruce	24	1.579	0.020	0.185	0.017	0.110	0.227
	40	2.517	0.055	0.358	0.047		

TABLE IIB Tabulation of the stress dependent values for Method 2 (e.g. Equations 12 to 16)

Material	σ (N mm^{-2})	$\hat{\epsilon}_{ir}$ (% at t = 1 sec)	$\hat{\epsilon}_m$ (% at t = 1 sec)	$\hat{\hat{\epsilon}}_r$ (% at t = 1 sec)	q	$\bar{q}$
Poured asphalt	0.2	0.720	0.416	0.165	0.323	0.341
	0.4	0.910	0.628	0.304		
Spruce	24	0.185	1.594	0.035	0.0112	0.0579
	40	0.358	2.640	0.143		

For one single loading, the total strain becomes

$$\epsilon_g = \hat{\epsilon}_{ir} + \hat{\epsilon}_m \cdot t^q, \tag{12}$$

with

$$\hat{\epsilon}_{ir} = \hat{\Phi}_{1ir}\sigma + \hat{\Phi}_{2ir}\sigma^2 \tag{13}$$

and

$$\hat{\epsilon}_m = \hat{\Phi}_{1m}\sigma + \hat{\Phi}_{2m}\sigma^2 \tag{14}$$

and, after unloading, considering that

$$\hat{\epsilon}_r = \hat{\hat{\epsilon}}_r(t-\tau)^{\bar{q}} \tag{15}$$

with

$$\hat{\hat{\epsilon}}_r = \hat{\Phi}_{1r}\sigma + \hat{\Phi}_{2r}\sigma^2, \tag{16}$$

the corresponding equation becomes (see Table IIB)

$$\epsilon_g = \hat{\epsilon}_{ir} + \hat{\epsilon}_m\,[t^q - (t-\tau)^q] + \hat{\hat{\epsilon}}_r(t-\tau)^q. \tag{17}$$

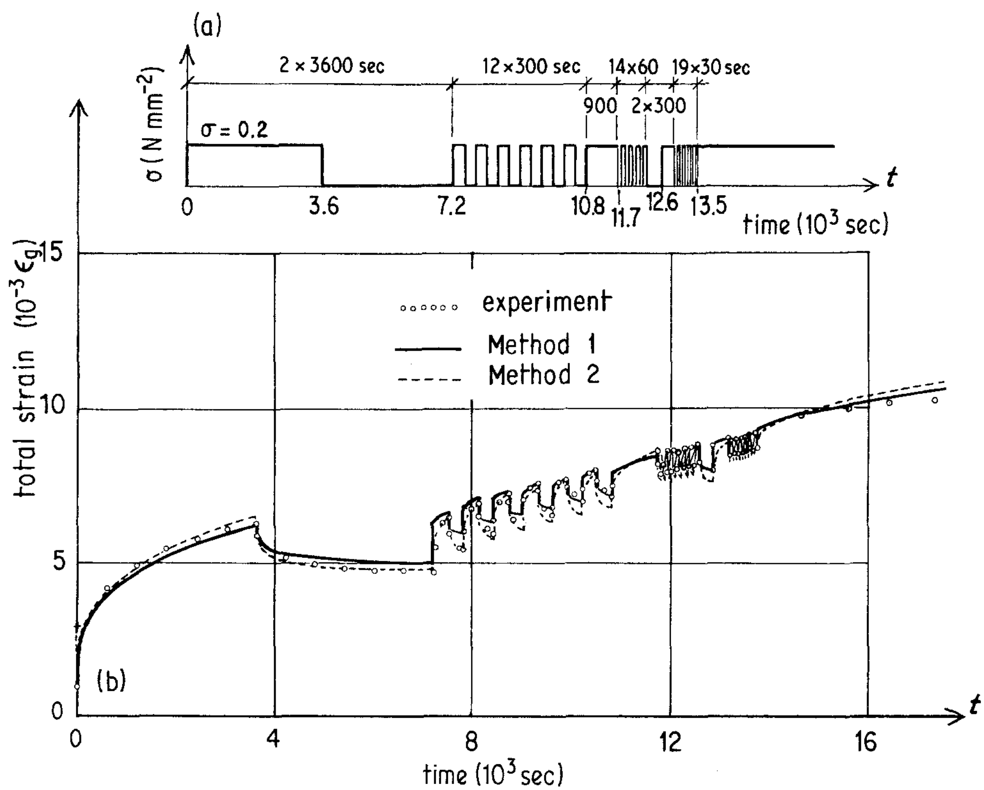

Figure 3 (a) Applied stress and (b) total axial strain of poured asphalt under arbitrary repeated single step-loading at 23° C and 50% r.h.

TABLE IA Tabulation of the material constants for Method 1

Material	Material constant									
	$\hat{\Phi}_{1e}$	$\hat{\Phi}_{2e}$	$\hat{\Phi}_{1ve}$	$\hat{\Phi}_{2ve}$	$\hat{\Phi}_{1p}$	$\hat{\Phi}_{2p}$	$\hat{\Phi}_{1vp}$	$\hat{\Phi}_{2vp}$	q_{ve}	q_{vp}
Poured asphalt	1.875×10^{-3}	-2.375×10^{-3}	0.915×10^{-3}	-1.275×10^{-3}	4.925×10^{-3}	-6.625×10^{-3}	1.415×10^{-3}	-0.875×10^{-3}	0.278	0.340
Spruce	7.044×10^{-5}	-0.019×10^{-5}	-0.330×10^{-7}	$+0.352 \times 10^{-7}$	58.72×10^{-7}	0.769×10^{-7}	-0.050×10^{-7}	$+0.294 \times 10^{-7}$	0.110	0.227

TABLE IB Tabulation of the material constants for Method 2

Material	$\hat{\Phi}_{1ir}$	$\hat{\Phi}_{2ir}$	$\hat{\Phi}_{1m}$	$\hat{\Phi}_{2m}$	$\hat{\Phi}_{1r}$	$\hat{\Phi}_{2r}$	q	$\bar{q}$
Poured asphalt	4.925×10^{-3}	-6.625×10^{-3}	2.590×10^{-3}	-2.550×10^{-3}	0.890×10^{-3}	-0.325×10^{-3}	0.323	0.341
Spruce	5.875×10^{-7}	0.769×10^{-7}	0.067×10^{-3}	-0.250×10^{-7}	-0.180×10^{-5}	1.344×10^{-7}	0.0112	0.0579

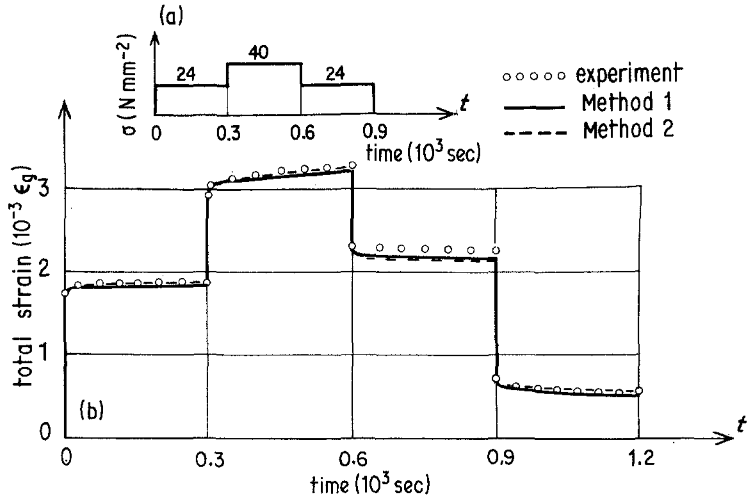

Figure 4 (a) Applied stress and (b) total axial strain of spruce under arbitrary step-loading at 23° C and 50% r.h. (moisture content of wood 11%).

The separation is based on the idea that, at the moment of spontaneous loading, an irreversible change in cohesion occurs (e.g., between the bituminous matrix and the minerals) since growing loading velocity generally increases the tendency of materials to behave in a stiffer manner. Thus, an irreversible strain ϵ_{ir} contributes to the total strain ϵ_g. The following constant loading from $t = 0$ to $t = \tau$ produces a time-dependent change in structure which, in turn, alters the mechanical behaviour with respect to the initial state. Thus, the change in mechanical behaviour is due to the spontaneous change in cohesion and due to a time-dependent structural change as well, both changes preventing total recovery. In order to predict the strain by the material functions of the initial loading, it is useful to introduce $\bar{\epsilon}_r$ as an auxiliary value for the third part of strain. If the loading cycle is repeated, further changes in structure occur which, however, decrease with higher number of loadings, N. Consequently, $\bar{\epsilon}_r$, as well as $\Delta\epsilon_{ir}$, i.e., the growth of irreversible spontaneous strain, tend to zero. The influence of increasing number of loading N on $\bar{\epsilon}_r$ and ϵ_m is obtained by separate application of the modified superposition principle. ϵ_{ir} can be obtained from

$$\epsilon_{ir} = \hat{\epsilon}_{ir}N^q, \tag{18}$$

assuming that the spontaneous irreversible strain shows a similar dependence on N as the creep strain, ϵ_m, on the time, t. The corresponding eight material constants are indicated in Table IB.

Fig. 8. illustrates the application of Method 2 to the same arbitrary loading history as in Fig. 2.

The total strain, $\epsilon_g = \epsilon_{g1} + \epsilon_{g21}$ can be calculated by separate superposition of ϵ_{ir}, $\bar{\epsilon}_r$ and ϵ_m. The time-dependent strain parts, $\bar{\epsilon}_r$ and ϵ_m, are determined by the modified superposition principle considering that $\bar{\epsilon}_r$, by definition, occurs only after the first time of loading at $t = \tau_2$.

3. Materials and test procedure

The uniaxial compression creep-tests were performed on poured asphalt and spruce in a standard climate at 23° C and 50% relative humidity (r.h).

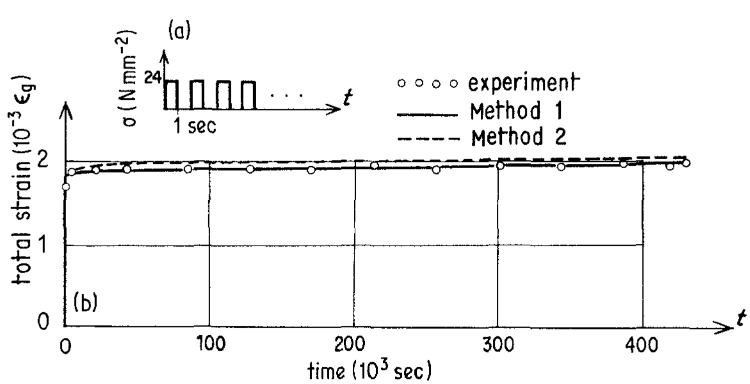

Figure 5 (a) Applied stress and (b) total axial strain of spruce at 23° C and 50% r.h. under repeated single step-loading (moisture content of wood 11%).

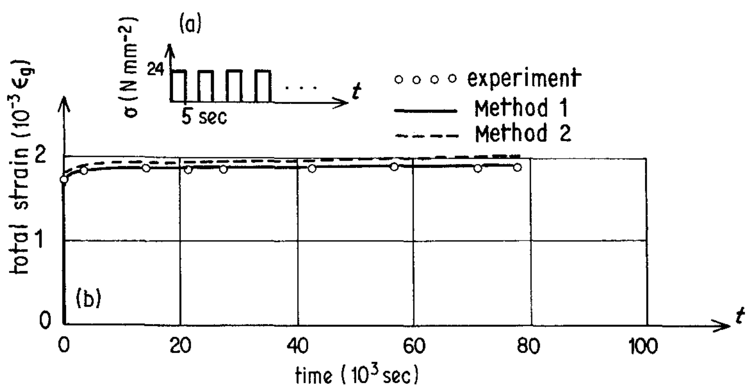

Figure 6 (a) Applied stress and (b) total axial strain of spruce at 23° C and 50% r.h. under repeated single step-loading (moisture content of wood 11%).

The poured asphalt had a binder content of 9 wt % B 40/50 and a mineral content of 91 wt % of grain size 0/6 mm. The mineral consisted of 25 wt % hard filler, 45 wt % sand 0/3 mm and 30 wt % crushed stone 3/6 mm. To obtain cylindrical specimens with a diameter of $\phi = 50$ mm and a height of 150 mm, moulds of two semi-circle brass segments were used, in which the mixture was filled and compressed at a temperature of about 230° C.

For the experiments on wood, prismatic specimens of European spruce (*Picea abies* (*L*) *Karst.*) were used, with the size of 50 mm x 50 mm x 150 mm. The average oven-dry density was 380 kg m^{-3} and the average moisture content 11%. The load was applied parallel to the fibres.

The experiments were performed on electronic testing machines. To measure the deformations of poured asphalt and spruce, linear-variable-differential-transformer (LVDT) extensometers were used. All experiments were performed with a small pre-load of a maximum of 1/10 of the creep load. The step-loading was applied within 1 sec.

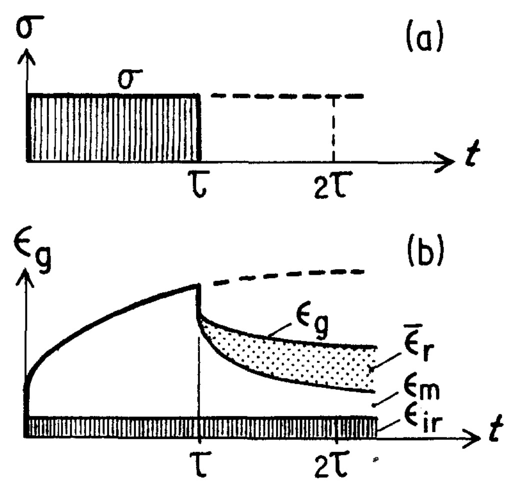

Figure 7 (a) Applied stress and (b) separation of the total resulting strain for Method 2 into: ϵ_{ir} (difference between the spontaneous strain increments at $t = 0$ and $t = 2\tau$); ϵ_m (strain calculated from $\epsilon_g - \epsilon_{ir}$ of the loading period by the modified superposition principle), and $\bar{\epsilon}_r$ (strain differnece in the recovery period between total strain ϵ_g and the calculated strains ϵ_m and ϵ_{ir}).

4. Results and discussion

In a first step the power functions of the individual strain parts were determined from the experimental creep functions under step-loading according to Method 1 (Fig. 1), and in a second step the strain parts were calculated according to Method 2 (Fig. 7). For this purpose, the time-dependent strain parts were plotted in a double logarithmic scale and approximated by straight lines, assuming that the slopes q_{ve}, q_{vp}, q, $\bar{q}$ of every single step-loading were equal for each strain part. The values $\hat{\epsilon}$ in Table II denote this strain parts at $t = 1$ sec and depend only on stress. The dependence was approximated by the polynomial Equations 5 to 9 for Method 1 and by Equations 12 to 17 for Method 2. The corresponding material constants $\hat{\Phi} \ldots$, as well as the slopes $q \ldots$, are listed in Table I. It has to be emphasized that these constants are limited to the specific samples and materials and may not be used for general construction purposes. This would require more extensive research and was not the aim of the present work.

The irreversible strains of poured asphalt are relatively large compared to the reversible strains, and the material shows a non-linear behaviour. Thus both methods are applied and checked with the experimental results of arbitrary loading histories. The loading history of Fig. 3 with an arbitrary combination of short- and long-time loading were chosen to demonstrate the sensitivity of both methods. Though the material constants are determined from experiments with compara-

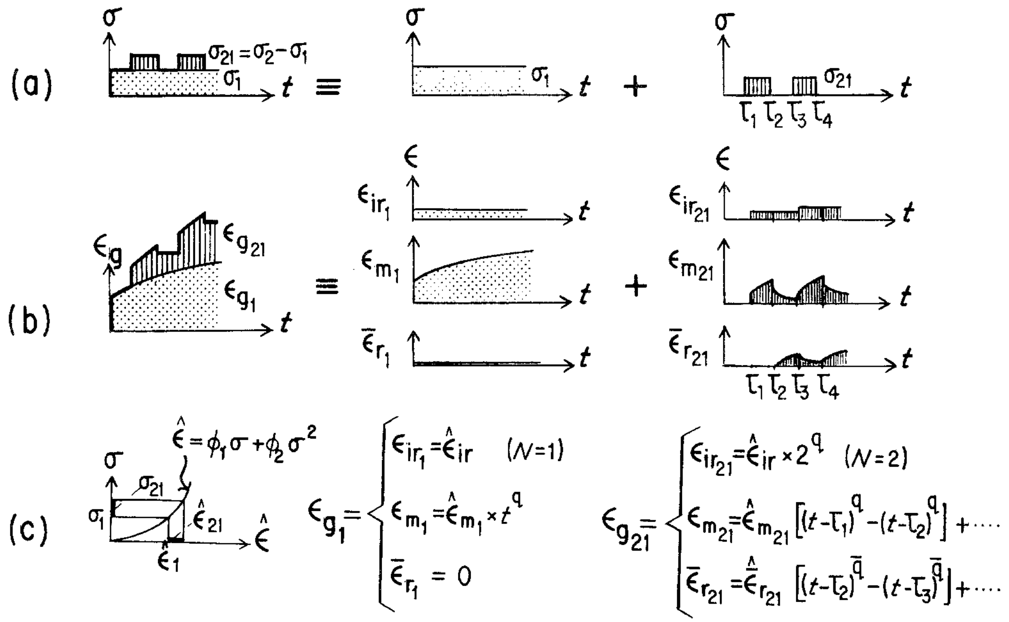

Figure 8 Example of the superposition according to Method 2. (a) Separation of the stress history in σ_1 and $\sigma_2 - \sigma_1 = \sigma_{21}$ (see Fig. 2); (b) separation of the total strain according to Figs 3 and 4c; (c) determination of non-linear constants $\hat{\epsilon} \ldots, q \ldots$ (Table II) and calculation of total deformation ϵ_{g_1} (Equations 12 to 14 and 18) and $\epsilon_{g_{21}}$ (e.g., Equations 17 and 18) with modified superposition principle for ϵ_m and $\bar{\epsilon}_r$ within the time period $t = 0 \ldots t$ and $t = \tau_2 \ldots t$, respectively.

tively long creep and recovery times both methods agree quite well and the difference to the measurements is small (see Table III). As expected, for Method 1 there is a maximum difference of spontaneous irreversible part at the second loading cycle. For Method 2 the recovery is overestimated with increasing number of loading cycles (see Table III). A comparison between these and some other approximate methods is given in [13]. It is

TABLE III Comparison between the predictions of Method 1 and 2 and experimentally determined values

Figure	Time	$\frac{\epsilon_{\text{theor}} - \epsilon_{\text{exp}}}{\epsilon_{\text{theor}}} \times 100$ (%)	
		Method 1	Method 2
Fig. 6	3600 sec	− 0.0	3.7
	7500 sec	2.4	0.0
	11000 sec	− 1.8	− 2.5
	13500 sec	0.0	− 2.9
	64800 sec	4.0	6.4
Fig. 7	10 min	− 2.0	− 1.2
	15 min	− 3.0	− 4.3
Fig. 8	24 h	0.0	4.8
	120 h	0.5	4.4
Fig. 9	4 h	0.0	3.5
	22 h	1.1	6.5

also shown that, in the case of Fig. 3, the application of Method 2 without introducing ϵ_{ir} (see Fig. 7) yields to a total strain which is 25% below the experimentally determined value.

The influence of non-linearity on the behaviour of spruce at a moisture content of 11% is less important as for example on poured asphalt (see values of Φ_1 and Φ_2 in Table II). The spontaneous irreversible strain part of initial loading is comparatively large and hardly increasing under repeated similar loading (see Figs 5 and 6). Hence, according to Methods 1 and 2, the spontaneous irreversible strain can be determined without Equations 10 and 18, i.e., without assuming a hardening effect with increasing number of loadings, N. Fig. 4 gives the comparison between theory and experiment for arbitrary step-loading. Figs 5 and 6 present the verification of the suggested methods for repeated single-step loading. The agreement with the experimental data is good (see Table III).

5. Conclusions

Two methods are presented to describe non-linear material behaviour at constant temperature. The first requires ten and the second eight material constants. In the case of linearity the number of constants reduces to four and three, respectively.

The first method [6] is based on the separate superposition of the irreversible and reversible time-dependent and time-independent strain parts; the second method [7] is founded on the superposition of an irreversible, reversible and retarded reversible strain part, the latter caused by the resistance against recovery.

It was shown that the behaviour of poured asphalt and spruce, both materials with more or less distinctive irreversible character, can be fairly well approximated by simple methods considering the behaviour of recovery.

References

1. B. WEHNER, P. SIEDEK and K. H. SCHULZE, "Handbuch des Strassenbaus" (Springer Verlag, Berlin, Heidelberg and New York, 1977) p. 123–127.
2. W. N. FINDLEY, J. S. LAI and K. ONARAN, "Creep and Relaxation of Non-linear Viscoelastic Materials" (North Holland Publishers, Amsterdam, 1976) p. 220–238.
3. F. J. LOCKETT, "Non-linear Viscoelastic Solids" (Academic Press, New York and London, 1972) p. 156–184.
4. R. M. CHRISTENSEN, "Theory of Viscoelasticity – An Introduction" (Academic Press, New York and London, 1971) p. 221–231.
5. J. D. FERRY, "Viscoelastic Properties of Polymers" (John Wiley and Sons, New York, 1980) p. 96–176.
6. A. C. TINIÇ, Dissertation, ETH, Zürich, (1978).
7. M. PARTL and A. C. TINIÇ, Report (Institut für Baustoffe, Werkstoffchemie und Korrosion, ETH, Zürich, 1979).
8. K. KRASS, Report N37 (Institute für straßen, Eisenbahn und Felsbar, ETH, Zurich 1977).
9. J. S. LAI and D. ANDERSON, Highway Research Record Number 478, (1974).
10. W. N. FINDLEY and G. KHOSLA, *J. Appl. Phys.* **26** (1955) 821.
11. W. N. FINDLEY and J. S. Y. LAI, *Trans. Soc. Rheol.* **11** (1967) 361.
12. A. C. TINIÇ and A. RÖSLI, *Bitumen* 3 (1980).
13. M. PARTL, Report (Institut für Baustoffe, Werkstoffchemie und Korrosion, ETH, Zürich, 1980).

Received 8 June
and accepted 18 August 1981